University of Nebraska - Lincoln
DigitalCommons@University of Nebraska - Lincoln

Norman R. Simon Papers | Research Papers in Physics and Astronomy

6-20-1993

A PROVISIONAL RR LYRAE DISTANCE SCALE

Norman R. Simon
University of Nebraska - Lincoln, nsimon@unl.edu

Christine M. Clement
University of Toronto, cdement@doncarlo.astro.utoronto.ca

Follow this and additional works at: https://digitalcommons.unl.edu/physicssimon

Simon, Norman R. and Clement, Christine M., "A PROVISIONAL RR LYRAE DISTANCE SCALE" (1993). *Norman R. Simon Papers*. 40.
https://digitalcommons.unl.edu/physicssimon/40

This Article is brought to you for free and open access by the Research Papers in Physics and Astronomy at DigitalCommons@University of Nebraska - Lincoln. It has been accepted for inclusion in Norman R. Simon Papers by an authorized administrator of DigitalCommons@University of Nebraska - Lincoln.

THE ASTROPHYSICAL JOURNAL, 410:526–533, 1993 June 20
© 1993. The American Astronomical Society. All rights reserved. Printed in U.S.A.

A PROVISIONAL RR LYRAE DISTANCE SCALE

NORMAN R. SIMON
Department of Physics and Astronomy, University of Nebraska, Lincoln, NE 68588-0111
AND
CHRISTINE M. CLEMENT
David Dunlap Observatory, Department of Astronomy, University of Toronto, Toronto, Ontario, Canada M5S 1A1
Received 1992 October 26; accepted 1992 December 17

ABSTRACT

Hydrodynamic pulsation models are matched with observations of globular cluster RR*c* stars to derive masses, luminosities and temperatures as functions of two observables: pulsation period, P_1, and Fourier phase parameter, ϕ_{31}. We find that mean RR*c* masses and luminosities increase, and mean temperatures fall, with decreasing cluster metallicity. The Oosterhoff dichotomy is explained as mainly a temperature effect, while hints of a new dichotomy (in RR*c* mass and luminosity) are found among certain Oo II clusters. A provisional RR Lyrae distance scale emerges for the RR*c* stars in the form of a relation between luminosity and the two observables, P_1 and ϕ_{31}. Finally, the scheme we propose passes three independent tests: (1) it reproduces the observed hierarchy of relative luminosity among a large sample of RR*c* stars in ω Centauri; (2) it yields mean RR*c* masses which are fully consistent with the RR*d* masses derived for the clusters M68 and M15; and (3) it gives an LMC distance modulus in agreement with that obtained by other methods.

Subject headings: galaxies: distances and redshifts — globular clusters: general — Magellanic Clouds — stars: distances — stars: oscillations — stars: variables: other (RR Lyrae)

1. INTRODUCTION

The cosmic distance scale constitutes one of the most fundamental problems in astronomy, a problem in which the study of pulsating stars has played an important role. While, historically, the classical Cepheids have served as the primary distance indicator, in recent years the RR Lyrae pulsators have also received considerable attention. These stars are of interest for the theories of stellar evolution and galactic structure, as well as the distance problem. In a recent paper, Saha et al. (1992) have discussed and summarized the use of RR Lyrae stars to find distance moduli of external galaxies. The techniques employed have given rise to a discrepancy with the Cepheid studies, in that the RR Lyrae distance moduli are smaller by about 0.3 for IC 1613 and the LMC, and about 0.1 for M31.

In the present work we derive a new (provisional) RR Lyrae distance scale based upon the Fourier phase parameter ϕ_{31}. Our results are subjected to three independent tests, including one involving the LMC. We find an RR Lyrae distance modulus of 18.5, in close agreement with the Cepheid distance to the LMC. The RR Lyrae parameters we obtain also have a number of other interesting implications, including a substantial intracluster mass spread, an explanation of the Oosterhoff dichotomy as temperature driven, and a possible further intercluster dichotomy (in mass and luminosity) among the RR*c* samples in Oo II clusters.

2. THE FOURIER PARAMETERS

In the method of Fourier decomposition (e.g., Simon 1988), the light curves of pulsating stars are fitted with a Fourier series

$$\text{mag} = A_0 + \sum_{j=1}^{n} A_j \cos(jwt + \phi_j), \quad (1)$$

and the light curve shape quantified in terms of the lower order coefficients, viz., $R_{j1} = A_j/A_1$, $\phi_{j1} = \phi_j - j\phi_1$ ($j = 1, 2, 3, 4$). This technique was applied to globular cluster RR*c* stars in a recent study by Clement, Jankulak, & Simon (1992, hereafter CJS), which focused on the phase parameter ϕ_{31}. The results of this study are summarized in the plot of ϕ_{31} versus log period shown in Figure 1. Here each symbol represents the observed properties of an RR*c* star, and the differing symbols denote different clusters as indicated in the figure caption. All of the Figure 1 data were given in CJS, with the exception of the "open squares" which represent seven stars in the extreme metal-poor cluster, M68. The latter data are taken from recent observations, described by Clement, Ferance, & Simon (1993). The M68 points are seen to fall very close to those of M15 (*solid triangles*), a cluster with very similar properties.

Despite considerable scatter, the data in Figure 1 show two clearly discernable trends (see also CJS): (1) within each cluster, there is an increase of ϕ_{31} with period; and (2) the clusters are segregated according to metallicity, such that, for given ϕ_{31}, the period lengthens as [Fe/H] gets smaller. In the present work we shall set ourselves the task of interpreting these two properties with the aid of linear and hydrodynamic pulsation models. It is in the process of this interpretation that a preliminary RR*c* distance scale will emerge.

3. HYDRODYNAMIC MODELS

Hydrodynamic RR*c* (i.e., first overtone) pulsation models were integrated for a wide range of masses and luminosities. Model properties, including periods and Fourier parameters, have been tabulated and are published elsewhere (Simon & Clement 1993). The calculations are similar to those described by Simon (1990a, hereafter S90a), except that OPAL opacities (Rogers & Iglesias 1992) were employed. The chemical composition (dictated by then available opacity tables) was $X = 0.7$ and $Z = 0.001$ or 0.0001. The values of M and $\log L$ (both solar units) were as follows: 0.55 $M_\odot$ ($\log L = 1.58, 1.62, 1.66, 1.70, 1.78$); 0.65 $M_\odot$ ($\log L = 1.66, 1.70, 1.74, 1.78, 1.82$);

© American Astronomical Society • Provided by the NASA Astrophysics Data System

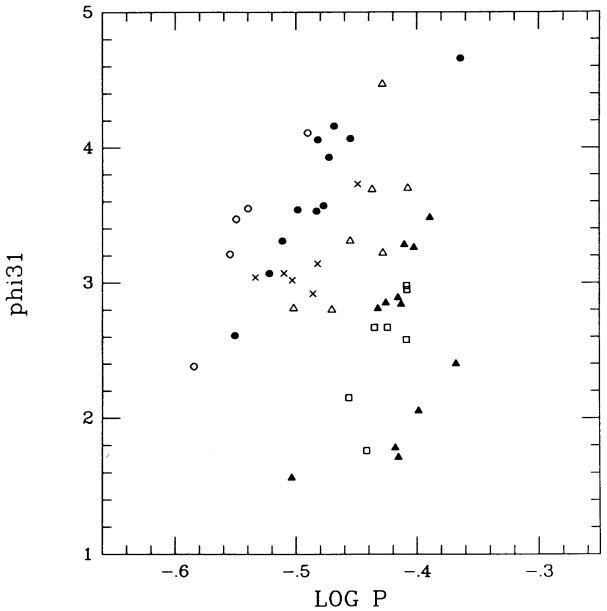

FIG. 1.—ϕ_{31} versus. log period for the RR_c stars in six clusters: NGC 6171 (*open circles*), M5 (*dots*), M3 (*crosses*), M53 (*open triangles*), M68 (*open squares*), and M15 (*filled triangles*).

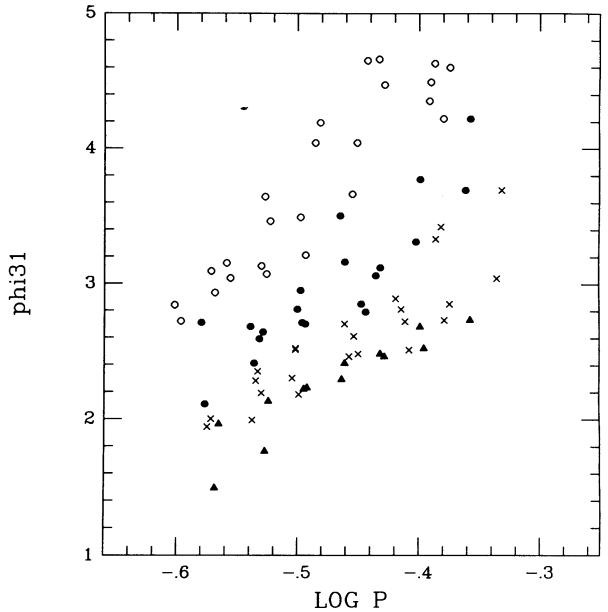

FIG. 2.—ϕ_{31} versus log period for four grids of hydrodynamic pulsation models: $M = 0.55\ M_\odot$ (*open circles*), $0.65\ M_\odot$ (*dots*), $0.75\ M_\odot$ (*crosses*), $0.85\ M_\odot$ (*filled triangles*).

$0.75\ M_\odot$ (log $L = 1.70, 1.74, 1.78, 1.82, 1.86, 1.90$); $0.85\ M_\odot$ (log $L = 1.70, 1.74, 1.78, 1.82, 1.86, 1.90, 1.94$).

For each pair (M, log L), two values of T_e were chosen, one near the first overtone blue edge and one near the fundamental mode blue edge. In this way, the first overtone instability region was crudely spanned (S90a). Each triplet (M, log L, T_e) was then integrated for each of the two metallicities, $Z = 10^{-3}$ and 10^{-4}. Thus, for each (M, log L) pair, four models were typically calculated, resulting in a total of over 80 models in all. The model integrations were continued for 100 to 300 periods to allow the light curves to settle down close to their limiting forms. The final light curves were then converted to magnitudes and fitted with equation (1), whereupon the ϕ_{31} value was extracted for each model.

The structure of the present models in general, and the ϕ_{31} values in particular, are very similar to those found by S90a who used Los Alamos opacities. The opacity law does not play a crucial role in determining ϕ_{31}. Nor does the metallicity. In the current study, pairs of models with identical parameters, but different metallicities, produce light curves whose ϕ_{31} values differ on the average by $|\delta\phi_{31}| = 0.2$. These small differences seem completely random (Simon & Clement 1993) and are likely caused by slightly different convergence properties in the various models, i.e., ϕ_{31} approaching its limiting value by a slightly different path. If this is the case, then the ϕ_{31} differences can be taken as a measure of the error in determining ϕ_{31} for a given hydro model: thus, $\Delta\phi_{31} \cong \pm 0.1$. This number is in accord with error estimates made in a different way by S90a.

Taken together, the present study and that of S90a comprise over 120 hydrodynamic pulsation models. The salient feature that emerges concerning the crucial phase parameter ϕ_{31} is that *ϕ_{31} depends essentially on mass and luminosity only, and is insensitive to metallicity, helium abundance, effective temperature and the choice of opacity law* (see also Simon 1989, 1990b). This property will enable us to generalize our models to a wider domain in the section which follows.

In Figure 2 we show the ϕ_{31} versus log period diagram for the current models. The different symbols denote different masses as indicated in the caption. For each mass, one observes a general increase of ϕ_{31} with period. In addition, the various masses are crudely segregated, with the smaller mass models lying higher in the diagram, i.e., displaying shorter periods at a given value of ϕ_{31}. This behavior is, of course, very reminiscent of that in Figure 1, with "stellar mass" replacing "cluster metallicity" as the distinguishing variable.

4. MODEL GENERALIZATION AND FITTING

We shall now extend the domain of our calculations, employing standard linear nonadiabatic (LNA) pulsation models. The reason for doing this is twofold: (1) at the time these calculations were made, OPAL opacities were available only for $X = 0.7$; and (2) the hydrodynamic integrations are, of course, very expensive compared with linear calculations. We shall return to this point in a later section.

Let us proceed as follows, taking into account the result, mentioned above, that ϕ_{31} is a function of mass and luminosity only. For each (M, log L) pair, we determine a single value of ϕ_{31} by averaging over all the hydro models calculated for that pair (see § 3). Then for each (M, log L) we calculate two linear models, one at the first overtone blue edge and one 50 K redward of the fundamental blue edge. This latter is done for three values of the helium abundance: $Y = 0.30, 0.25$ and 0.20. Since the blue edges shift when Y is changed, the models, of course, get cooler as Y gets smaller. In this way, we again attempt to span the first overtone instability region with two models for each (M, log L, Y). This procedure results in a total of about 140 models, each characterized by the parameter set: M, log L, Y, T_e, ϕ_{31} and P_1, where the overtone period P_1 is obtained from the LNA calculation.

We now make fits to the model sample, obtaining the following two relations:

$$\log T_e = 3.265 - 0.3026 \log P_1 - 0.1777 \log M + 0.2402 \log L \quad (2)$$

© American Astronomical Society • Provided by the NASA Astrophysics Data System

and

$$\log Y = -20.26 + 4.935 \log T_e - 0.2638 \log M + 0.3318 \log L . \quad (3)$$

Equation (2) is just a version of the familiar period/mean-density pulsation law, while equation (3) describes how the mean locus of the first overtone instability strip changes with helium abundance.

It now remains to introduce the key quantity, ϕ_{31}. It is not obvious a priori how to do this; in fact, three fitting schemes seem equally logical here. We present the results in what follows.

CASE A

$$\begin{cases} \log M = 0.571 + 0.610 \log P_1 - 0.113\phi_{31} + 0.200 \log Y & (4a) \\ \log L = 1.645 + 0.137\phi_{31} + 1.770 \log M; & (5a) \end{cases}$$

CASE B

$$\begin{cases} \log L = 2.829 + 1.311 \log P_1 - 0.0754\phi_{31} + 0.405 \log Y & (4b) \\ \log M = -0.813 - 0.0777\phi_{31} + 0.499 \log L; & (5b) \end{cases}$$

CASE C

$$\begin{cases} \log M = 0.571 + 0.610 \log P_1 - 0.113\phi_{31} + 0.200 \log Y & (4c) \\ \log L = 2.829 + 1.311 \log P_1 - 0.0754\phi_{31} + 0.405 \log Y . & (5c) \end{cases}$$

As indicated, we have called the above schemes Cases A, B and C, respectively. We note that equations (4c) and (5c) are merely reprises of equations (4a) and (4b). However, their combination makes a new case, which we have indicated separately, for clarity. Each of the cases A through C represents a different way of fitting the 140 models described above. In each of these fits we put the independent (i.e., observed) variables, $\log P_1$ and ϕ_{31}, together on the right, and the variables to be determined, $\log M$ and $\log L$, alone on the left. This best mimics the actual process of deriving the fundamental parameters of the RR*c* stars.

Before going on to apply our equations to observed stars, it is necessary to say a word about the quantity Y. While we have introduced it as the "helium abundance," henceforth we shall refer to Y more accurately as the *helium parameter*. The reason is as follows. It is well-known that the calculated blue edges, while dependent on the helium abundance, are also influenced by various uncertainties in the codes, e.g., those regarding boundary conditions and the treatment of convection. We have varied only the helium abundance to shift the blue edges, but actually, it makes sense to combine all of the uncertainties in the parameter Y. Thus a higher value of Y determined for a given cluster will mean hotter blue edges, either because helium is really more abundant in the ionization zones of RR*c* stars in that cluster, or because correct physics and numerics in the codes *would* yield hotter blue edges, or both. A lower value of Y denotes the opposite. The question of the true helium abundance is a difficult one, involving such complex phenomena as mixing during the helium flash, mass loss and, possibly, gravitational settling. Thus, the values we shall ultimately derive do not necessarily correspond to actual abundances in the ionization zones (although they might) and certainly should not be taken as an accurate indication of the main-sequence helium abundances, and still less of primordial helium.

However, although the absolute values of Y derived for the various clusters should not necessarily be taken literally, the *relative* values perhaps will deserve more credence. This is because changes in code physics and numerics are less likely to move the blue edges differentially, than to change them by a (more or less) fixed amount at all masses and luminosities. The actual value of Y in the ionization zones still seems the most important input which could determine why one cluster's instability strip is hotter or cooler than another's.

Let us make one final note before ending this section. The LNA calculations referred to above were made with Los Alamos opacities (Stellingwerf fit), those having been the only available for $X \neq 0.7$. It is known that the opacity law slightly influences the blue edge temperatures (Kovács, Buchler, & Marom 1991), but by an amount ($\sim$50 K) which is smaller than other uncertainties in the calculations. In any event, the parameter Y was specifically introduced to subsume all such uncertainties.

5. DERIVED PROPERTIES OF RR*c* STARS

Equations (2) and (3) along with any one of the pairs (4a, 5a), (4b, 5b) or (4c, 5c) constitute a set which may be solved for the derived variables $\log M$, $\log L$, $\log T_e$ and $\log Y$ in terms of the observables, $\log P_1$ and ϕ_{31}. This process is discussed further in § 10, below. Because the relations we obtain are linear, they may be applied both to individual RR*c* stars and to cluster averages. Table 1 shows average RR*c* masses and luminosities for six clusters (five from CJS plus M68), derived for Cases A, B and C, respectively. We note that the three cases yield similar values, the main difference being the slightly larger (smaller) luminosities emerging from Case A for clusters with higher (lower) metallicity.

Because we do not know which case to prefer, we shall merely average them, calling the result the "Combined Case" (see § 10). This leads to Table 2, in which we have also displayed derived values for the helium parameter, Y, and the average effective temperature of the RR*c* stars. Published values of metallicity for the various clusters are also included for convenience. While the data in Table 2 provide the basis for considerable discussion, we shall defer this to a later section. First, we would like to subject our results to a number of independent tests.

TABLE 1

MEAN CLUSTER PARAMETERS ACCORDING TO CASES A, B, AND C

	CASE A		CASE B		CASE C	
CLUSTER	$\langle M \rangle$	$\langle \log L \rangle$	$\langle M \rangle$	$\langle \log L \rangle$	$\langle M \rangle$	$\langle \log L \rangle$
NCG 6171	0.58	1.67	0.56	1.64	0.56	1.64
M5	0.57	1.71	0.56	1.69	0.56	1.69
M3	0.63	1.72	0.62	1.71	0.63	1.71
M53	0.62	1.75	0.62	1.75	0.62	1.75
M68	0.79	1.81	0.80	1.83	0.80	1.83
M15	0.79	1.81	0.81	1.84	0.80	1.84

© American Astronomical Society • Provided by the NASA Astrophysics Data System

TABLE 2

MEAN CLUSTER PARAMETERS ACCORDING TO "COMBINED CASE"

Cluster	[Fe/H]	Y	$\langle M \rangle$	$\langle \log L \rangle$	$\langle T_e \rangle$
NGC 6171	−0.99	0.30	0.57	1.65	7420
M5	−1.40	0.28	0.56	1.70	7300
M3	−1.66	0.28	0.63	1.71	7280
M53	−2.04	0.27	0.62	1.75	7190
M68	−2.09	0.24	0.79	1.82	7070
M15	−2.17	0.24	0.80	1.83	7050

6. THREE TESTS

6.1. log L *versus Observed Magnitude*

Let us now apply the Combined Case (average over Cases A, B and C) to the individual RR*c* stars in a given cluster, calculating for each star a value of log L (see also, Simon & Clement 1993). We may also obtain observationally for each star, a mean magnitude averaged over the pulsation cycle. This is just the "A0 term" in the Fourier decomposition [see eq. (1) and CJS]. While log L and A0 are gotten by totally independent means, they must, of course, be closely related since both reflect the relative luminosities of the stars.

Figures 3*a* and 3*b* show plots of log L versus observed magnitude in each of the six clusters we have treated. While several of the cluster plots show possible signs of correlation, others look more like scatter diagrams. Of course, there are considerable uncertainties in the determination of both log L and A0 for individual stars. It is interesting to note that while errors in the former quantity should be random, the potential exists for a systematic error in determining A0 for certain objects. This will occur when crowding in the field adds a constant light. In that event, to first approximation, the light curve ought to appear anomalously bright while ϕ_{31} remains largely unaltered. We have performed some simulations which show that this is indeed the case. The result is a situation where log L, determined from ϕ_{31}, is not affected, but A0 is too bright.

The plot for M5 (Fig. 3*b*) is interesting in this regard. The three stars with brightest observed magnitudes are just the three members of the M5 sample which lie closest to the center of the cluster, where crowding effects are most likely. Reducing their observed light by 0.2 mag would move them among the other stars in the M5 plot, making a log L − A0 correlation more plausible. A simple calculation shows that a crowding effect of this magnitude would require an extra luminosity in the field, equal to about 20% of the RR Lyrae star's actual luminosity. Finally, there is in the M5 plot one other object which seems too bright for its derived luminosity: this is the point at log $L \sim 1.68$, A0 ~ 15.2. This star is an outlier, located far from the cluster center; if it were actually also 0.1 mag in the foreground, this would move its point appropriately leftward in Figure 3*b*.

Be that as it may, one must say that the evidence provided by Figures 3*a* and 3*b* seems inconclusive: the uncertainties in the data tend to overwhelm the small samples. Future observations using CCD detectors could make these tests more effective. However, there does exist a cluster with a large RR*c* data set, namely ω Centauri (Simon 1989, 1990b; CJS). Figure 4 shows the ϕ_{31}-log period diagram for the ω Cen RR*c* stars (*star symbols*), with the stars from NGC 6171 (*open circles*). M5 (*dots*) and M68 (*open squares*) included for reference. The ω Cen points come from the data of Martin (1938) as analyzed by Petersen (1984). One sees that the ω Cen stars span practically the entire range of the other clusters.

In Figure 5 we plot log L versus A0 for the 47 star ω Cen RR*c* sample of Figure 4. The log L-values were determined using the Combined Case as described above. Figure 5 exhibits a definite correlation between log L and A0. A linear fit to the data yields a slope of 0.26, with standard deviation 0.026 in log L. This latter number is fully in line with the uncertainties in the method (see below). When the four points with brightest A0

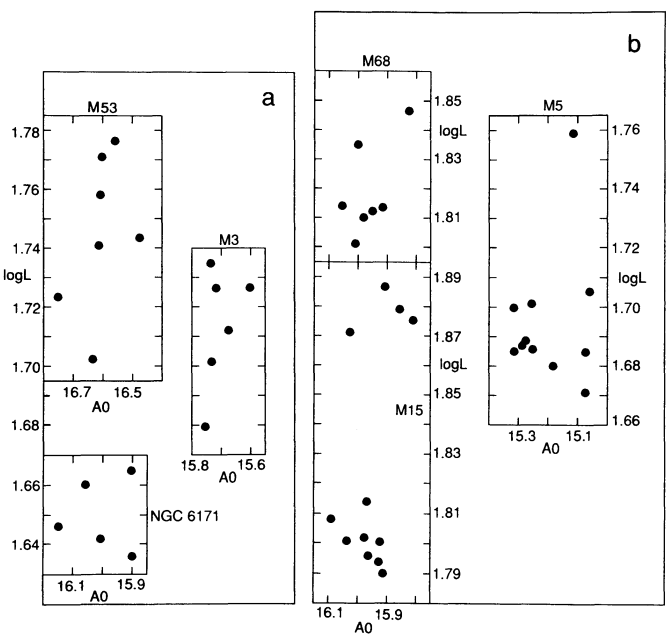

FIG. 3.—Inferred luminosity (log L) vs. observed mean magnitude (A0) for individual RR*c* stars in six clusters, as labeled: (*a*) M53, M3, NGC 6171; (*b*) M68, M5, M15.

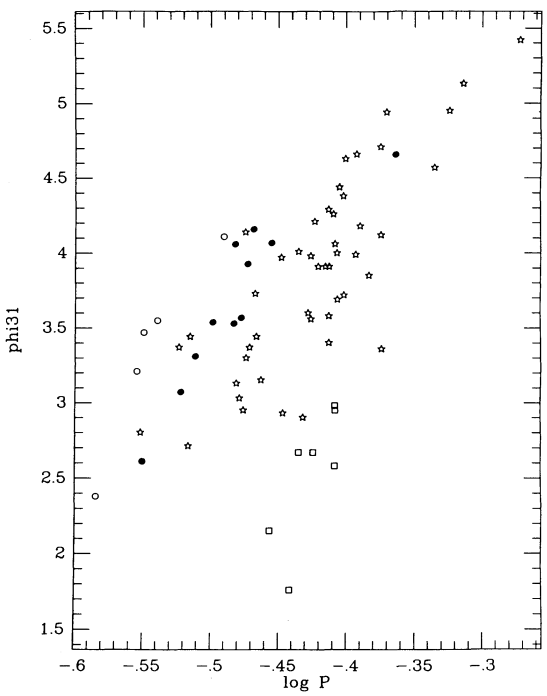

FIG. 4.—ϕ_{31} vs. log period for 47 RR*c* stars in ω Centauri (*stars*). Data for NGC 6171 (*open circles*), M5 (*dots*), and M68 (*open squares*) are included for comparison.

© American Astronomical Society • Provided by the NASA Astrophysics Data System

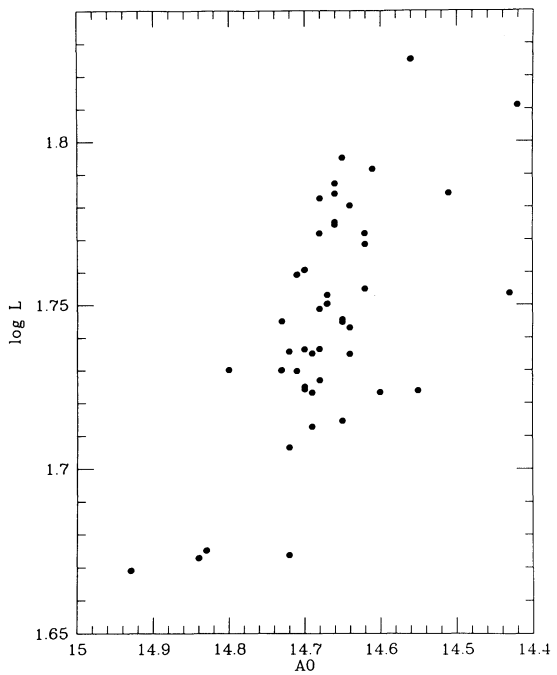

FIG. 5.—Inferred luminosity (log L) vs. observed mean magnitude (A0) for 47 RRc stars in ω Centauri.

are removed from the sample (once more invoking potential crowding effects to account for their departure from the main trend), the slope becomes 0.37, very close to the expected value 0.40, which defines the log L-magnitude relation. We take Figure 5 to constitute strong evidence that our method cannot be too far off base.

6.2. *The* RR*d stars*

The RRd stars pulsate simultaneously in the fundamental and first overtone modes. Two of the clusters we have treated contain substantial numbers of these objects. We have extracted RRd samples of eight stars from M15 (Nemec 1985; Clement & Walker 1990) and six stars from M68 (Clement et al. 1993), respectively. Given the pulsation periods, it is possible to infer the mass of an RRd star—or, strictly speaking, the mass as a function of luminosity, since the value one obtains depends somewhat upon the location one assumes for the star in the instability strip.

We have employed the fitting formula of Kovács et al. (1991), with $Z = 10^{-4}$, to obtain mean mass as a function of mean luminosity for the RRd samples in M15 and M68 (see Clement et al. 1993). The results are portrayed by the curves in Figure 6. Thus, for example, reading from the figure, if the mean luminosity of the RRd sample in M68 is $\langle \log L \rangle \sim 1.82$, then the mean mass is $\langle \log M \rangle \sim -0.10$, etc.

The crosses in Figure 6 denote the mean mass and luminosity of *the* RRc *stars* in each cluster, as determined by the Combined Case and listed in Table 2. It is clear that the derived RRc mass and luminosity in these two clusters is fully consistent with the RRd data, i.e., the crosses fall very near the curves. Furthermore, if we determine mean temperatures for the RRd stars, based upon their periods and the mass and luminosity values in proximity to the crosses in Figure 6 (i.e., $\langle \log L \rangle \sim 1.82$, $\langle M \rangle \sim 0.80$), the result is $6800 \lesssim \langle T_e \rangle \lesssim 6900$ K (Clement et al. 1993), i.e., the RRd stars in the two clusters lie

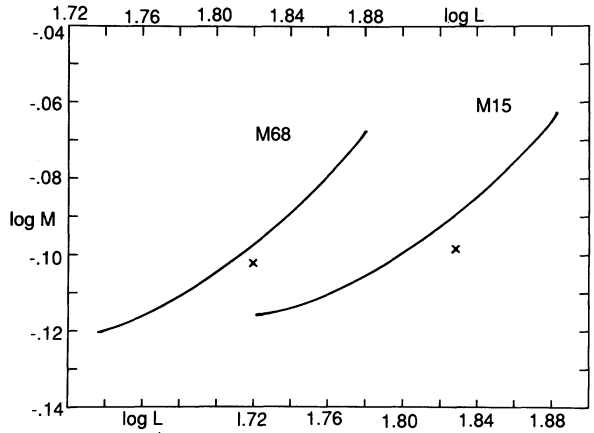

FIG. 6.—Inferred mean mass as a function of assumed mean luminosity for the RRd samples of M68 and M15 (*solid curves*, as indicated). *Upper abscissa*: M68; *lower abscissa*: M15. Crosses indicate mean parameters for the RRc samples in the respective clusters, as given in Table 2.

about 200 K redward of the RRc stars (see Table 2). This is just as one would expect (e.g., Cox, Hodson, & Clancy 1983).

6.3. *The LMC*

In a recent series of papers, A. R. Walker has published CCD photometry for RR Lyrae stars in a number of clusters in the Large Magellanic Cloud. We have examined the RRc light curves and, using the criteria described by CJS, found seven stars suitable for Fourier decomposition—four in the LMC cluster NGC 1841 (Walker 1990) and three in the Reticulum system (Walker 1992a). Walker himself has published ϕ_{31} values for all but one of these stars, V77 in the Reticulum.

In Figure 7 we plot the LMC stars on the ϕ_{31} versus log period diagram, with the M5 and M68 points included for reference. As with the Galactic stars, one notices the crude increase of ϕ_{31} with period within each LMC cluster. The locus for each cluster is roughly appropriate to its quoted metallicity, but our analysis would perhaps have the culum slightly more metal-poor than Walker's value of [Fe/H] = −1.7, and NCG 1841 slightly more metal-rich than Walker's value of [Fe/H] = −2.2.

Walker (1992b) has also discussed the question of the LMC distance modulus. He concludes that three independent lines of evidence (from Cepheids, from young and intermediate-aged clusters and from the SN 1987A interstellar ring) all converge on a distance modulus of 18.5 ± 0.1.

Results of applying the Combined Case (see § 10 for explicit equations) to the two LMC clusters are given in Table 3 (where we have also listed the result for ω Centauri, see § 6.1). Unfortunately, we cannot probe the LMC distance modulus with NGC 1841, since that cluster is generally acknowledged to lie a few tenths of a magnitude in the foreground (Walker 1990); we also find it to be so. However, in the case of the Reticulum, let

TABLE 3

MEAN PARAMETERS FOR LMC CLUSTERS AND ω CENTAURI

Cluster	{Fe/H}	Y	$\langle M \rangle$	$\langle \log L \rangle$	$\langle T_e \rangle$
NGC 1841	−2.2	0.26	0.70	1.76	7170
Reticulum	−1.7	0.27	0.67	1.74	7220
ω Cen	−1.6[a]	0.27[a]	0.58	1.75	7170

[a] Average over entire sample. Quantity varies from star to star.

© American Astronomical Society • Provided by the NASA Astrophysics Data System

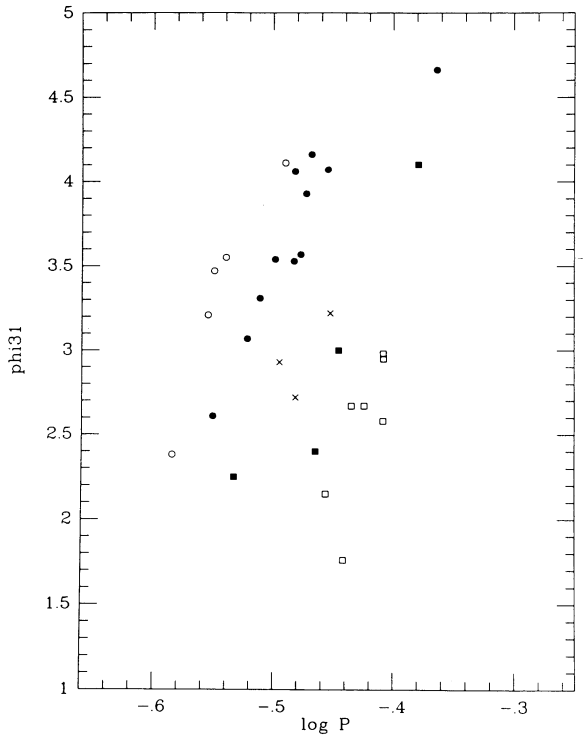

FIG. 7.—ϕ_{31} vs. log period for two LMC clusters: Reticulum (*crosses*), NGC 1841 (*filled squares*). Data for NGC 6171 (*open circles*); M5 (*dots*) and M68 (*open squares*) are included for comparison.

us take the mean luminosity given in Table 3 and convert it to an absolute visual magnitude using the Sandage & Cacciari (1990) formula (their eq. [7]). We obtain: $\langle M_V \rangle = 0.437$. The mean apparent visual magnitude for the three RR*c* stars is $\langle V \rangle = 19.07$, which becomes $\langle V \rangle_0 = 18.98$ when reddening is corrected following Walker (1992a). Finally $\langle V - M_V \rangle_0 = 18.54$, in close agreement with the value obtained by other methods.

7. MAGNITUDE AND METALLICITY

Figure 8 presents a plot of mean absolute visual magnitude versus [Fe/H] for the RR*c* samples in eight globular clusters—six from the galaxy (*dots*; see Table 2), and two from the LMC (*crosses*; see Table 3). The M_v-values are calculated from the

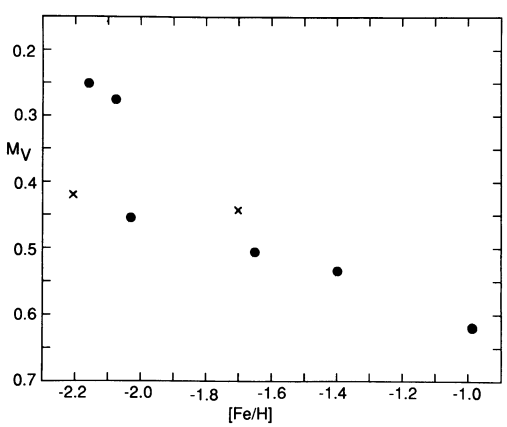

FIG. 8.—Inferred mean RR*c* absolute visual magnitude vs. published cluster metallicity: Galaxy (*dots*), LMC (*crosses*).

values of log L in Tables 2 and 3, respectively, again using the bolometric correction formula of Sandage & Cacciari (1990). A straight line fit to the six lowest lying points in Figure 8 yields a slope near 0.2, the value favored by many authors; on the other hand, ignoring M53 and NGC 1841 (*dot and cross at lower left*), produces a slope of about 0.3, closer to the larger value favored by others (see Sandage & Cacciari 1990 for a summary). Lacking more data, it is difficult to tell which slope (if either) ought to be preferred. However, Figure 8 does appear to indicate a dichotomy at low metallicity between M15 and M68, on the one hand, and M53 and NGC 1841 on the other. This is not the Oosterhoff dichotomy, since all four clusters are ostensibly Oo II. It remains to be seen, again pending additional data, whether or not this suggested division is real.

8. THE OOSTERHOFF DICHOTOMY AS A TEMPERATURE EFFECT

The Oosterhoff dichotomy between the longer period RR Lyraes in Oo II clusters and the shorter period RR Lyraes in Oo I clusters has been with us a long time and is still not well understood (see, e.g., the review by Rood 1990). The usual fiducial pair for illustrating the effect is M15 and M3. However, in the present discussion we shall choose M68 and M5, which have better data.

Let us first solve equation (2) for the period, and differentiate to obtain

$$\Delta \log P_1 = (-0.587 \Delta \log M + 0.794 \Delta \log L) - 3.305 \, \Delta \log T_e .$$

Then, applying this relation in the sense M68 *minus* M5, we have from Table 2,

$$\Delta \log P_1 = (-0.089 + 0.098) + 0.045 ,$$

where the three numbers on the right-hand side give the contributions from mass, luminosity and temperature, respectively. One notes that the mass and luminosity terms are each larger in absolute value than the temperature term, but that the former two largely cancel, leaving the latter to dominate—in this case producing about 84% of the period shift. In the case of M53 *minus* M5, the temperature contribution is about 61%, but this result is less trustworthy due to the lower accuracy of the M53 data.

In any event, if the numbers in Table 2 are correct, two conclusions emerge: (1) the RR*c* stars in clusters like M15 and M68 have longer periods than do those in, say, M5 and M3, due to cooler temperatures in the former stars, perhaps because a moderate lack of helium in the ionization zones has pushed their instability strips redward; and (2) it is not correct to formulate a period shift at constant temperature (e.g., Sandage 1982), since the instability strips of, say, M68 and M5 barely seem to overlap.

9. QUESTIONS AND UNCERTAINTIES

The first question we wish to raise concerns the hydrodynamic models. These models have a mixed record in mimicking the observed characteristics of RR Lyrae pulsations. The first overtone calculations generally reproduce the light curve shapes of the RR*c* stars (Simon 1990a) and, in particular (as the present work shows), seem to model ϕ_{31} quite satisfactorily (see also, Simon 1989, 1990b). On the other hand, these calculations are less than completely successful in mimicking the observed values of the Fourier parameter ϕ_{21} (Simon 1990a). In the case of the fundamental mode, the hydrodynamic inte-

© American Astronomical Society • Provided by the NASA Astrophysics Data System

grations are inadequate for both ϕ_{21} and ϕ_{31} (Simon 1985; Simon & Aikawa 1986). In addition, current models are far from satisfactory in reproducing observed double mode RR Lyraes (RR*d* stars), although some recent calculations may be more promising in this regard (Kovács 1993; Bono 1993).

In discussing the models, we should also recall that we have made actual nonlinear calculations with OPAL opacities only for $X = 0.7$ (see §§ 3 and 4 above). While there is much reason for believing that our procedure for generalizing these calculations is correct, additional hydro calculations for other abundances would certainly be desirable. However, given the amounts of computer time necessary to construct a large model grid, we deem it advisable to postpone such calculations for a short time, until the next generation of hydrodynamic codes (see, e.g., Kovács 1993) becomes available. Such codes may also be effective in ameliorating some of the problems that current models have in matching the observations (see above).

A second question that needs further discussion is that of the masses of the RR*d* stars. In § 6.2 above, it was shown that the RR*c* masses we have derived for stars in M68 and M15 are very consistent with independently determined RR*d* masses for the same clusters. For these extreme metal-poor clusters, the uncertainty in the latter masses due to lack of precise knowledge of chemical composition is relatively small, of the order $\pm 0.05\ M_\odot$ (Cox 1991; Kovács et al. 1991; Simon & Clement 1993). However, this is not the case for Oo I clusters. According to Table 2, the mean RR*c* mass for the Oo I cluster, M3, is $0.63\ M_\odot$. While this is considerably smaller than the Oo I RR*d* mass derived by Kovács et al. ($0.78\ M_\odot$), the composition-driven uncertainty in this latter mass is very large (Kovács et al. 1992). In fact, it has recently been argued (Cox 1993) that the Oo I RR*d* mass is actually $0.65\ M_\odot$, very close to the value we have obtained for the RR*c* sample in M3. The specific case of M3 probably cannot be considered critical, since this cluster contains only two RR*d* stars (Nemec & Clement 1989) out of a total RR Lyrae sample of about 180. Thus it could always be argued that these RR*d* stars have extreme masses which lie in the tail of the RR Lyrae distribution in M3. In this regard, the cluster IC 4499 is much more compelling, possessing 13 RR*d* stars out of about 80 total RR Lyraes (Clement et al. 1986). If the quoted metallicity, [Fe/H] = −1.38, is correct for this cluster, an RR*d* mass is considerably higher than $0.65\ M_\odot$ is probably indicated. It remains to be seen what the ϕ_{31}-based RR*c* mass will turn out to be for IC 4499—at present, the observations are not adequate to determine it.

In any event, the scheme we advocate for finding RR Lyrae masses and luminosities can certainly be tested further. Castellani & Quarta (1987) list 16 globular clusters containing eight or more RR*c* stars. CCD observations of these clusters (including IC 4499 and the six clusters we have treated) could produce a much larger and more accurate (provided that the phase coverage were good) data set that could be used to alter or embelish our preliminary conclusions. In addition, light curves adequate for finding ϕ_{31} could be obtained for many more RR*c* stars in the LMC. Such data would immediately test the consistency of our method, since the RR*c* stars from different LMC clusters would be expected to yield a single distance to the galaxy. We would welcome such data and such tests of our scheme.

Finally, we wish to say a few words about the uncertainties inherent in determining masses and luminosities from ϕ_{31}. The error in getting ϕ_{31} from the hydrodynamic models has been estimated above as $\Delta\phi_{31} = \pm 0.1$. The standard deviations of our linear fits to the hydro model output are typically 0.025 in $\log M$ (eqs. [4a], [4b], and [4c]) and 0.035 in $\log L$ (eqs. [5a], [5b], and [5c]). With respect to the observations we have employed, typical uncertainties in ϕ_{31} are between 0.3 and 0.4 (see CJS), while the uncertainties in the measured periods (both theoretical and observational) are essentially zero. While all of these uncertainties seem to be strictly random, we have not attempted to combine them into a formal error, so as to avoid quoting a number whose meaning in the real world would remain unclear. In particular, we are not at present confident in trying to calculate the uncertainty in mean masses and luminosities derived for the various clusters. This question should be more amenable to solution when larger and more extensive data sets become available.

10. A PROVISIONAL DISTANCE SCALE

To obtain expressions for mass and luminosity, we may solve equations (2) and (3) with any of the three sets: (4a, 5a), (4b, 5b), (4c, 5c). The various sets yield different solutions, which we write formally as

$$(\log M)_i = a_i \log P_1 + b_i \phi_{31} + c_i$$

$$(\log L)_i = d_i \log P_1 + e_i \phi_{31} + f_i ,$$

where $i = 1, 2, 3$, corresponding to the three sets.

Since, as indicated earlier, we do not know which set to prefer, we shall merely average each of the coefficients, e.g. $a = \sum_i a_i/3$, obtaining finally

$$\log M = 0.52 \log P_1 - 0.11\phi_{31} + 0.39 , \quad (6)$$

$$\log L = 1.04 \log P_1 - 0.058\phi_{31} + 2.41 , \quad (7)$$

where $\log P$ and ϕ_{31} are observed values for a given RR*c* star, or *preferably cluster averages for an ensemble of* RR*c stars*. The provisional RR Lyrae distance scale is then embodied in equation (7), while equations (2), (3), (6), and (7) together give rise to the entries in Table 2.

Simon & Clement (1993) have shown that *intracluster* slopes on the ϕ_{31} versus log period diagram (Fig. 1) are reproduced very well by equation (7), provided that $\log L \sim$ constant among the RR*c* stars within a given cluster. On the other hand, their analysis also demonstrates that equation (6) implies a substantial intracluster mass range, perhaps of the order $0.1\ M_\odot$. These properties lead to a characterization of the RR*c* domain on the horizontal branch of a given cluster as narrow in luminosity (and temperature), but with a considerable spread in mass, the latter responsible for much of the observed *intracluster* period spread. With regard to the family of clusters, Table 2 shows a substantial range in *intercluster* temperature and luminosity as well as in mass.

These results give rise to many further questions, including that of a possible discrepancy between the masses and luminosities given in Table 2 and those emerging from calculations of horizontal branch evolution (e.g., Lee & Demarque 1990). While such a discrepancy may exist, its magnitude will depend upon the details of the evolution calculation, including the chemical abundances that are assumed. A careful study of these and other problems is beyond the scope of the present work and must be left to the future.

We are pleased to acknowledge the aid of S. M. Kanbur in making some of the calculations described in this article. Also, we are grateful for financial support from the NASA Astrophysics Theory Program (NRS), and the Natural Sciences and Engineering Research Council of Canada (CMC).

© American Astronomical Society • Provided by the NASA Astrophysics Data System

REFERENCES

Bono, G. 1993, in New Perspectives on Stellar Pulsation and Pulsating Variable Stars, ed. J. M. Nemec & J. M. Matthews (Cambridge: Cambridge Univ. Press), 266
Castellani, V., & Quarta, M. L. 1987, A&AS, 71, 1
Clement, C. M., Ferance, S., & Simon, N. R. 1993, ApJ, submitted
Clement, C. M., Jankulak, M., & Simon, N. R. 1992, ApJ, 395, 192 (CJS)
Clement, C. M., Nemec, J. M., Robert, N., Wells, T., Dickens, R. J., & Bingham, E. A. 1986, AJ, 92, 825
Clement, C. M., & Walker, I. R. 1991, AJ, 101, 1352
Cox, A. N. 1991, ApJ, 381, L71
———. 1993, in New Perspectives on Stellar Pulsation and Pulsating Variable Stars, ed. J. M. Nemec & J. M. Matthews (Cambridge: Cambridge Univ. Press), 232
Cox, A. N., Hodson, S. W., & Clancy, S. P. 1983, ApJ, 266, 94
Kovács, G. 1992, in New Perspectives on Stellar Pulsation and Pulsating Variable Stars, ed. J. M. Nemec & J. M. Matthews (Cambridge: Cambridge Univ. Press), in press
Kovács, G., Buchler, J. R., & Marom, A. 1991, A&A, 252, L27
Kovács, G., Buchler, J. R., Marom, A., Iglesias, C. A., & Rogers, F. J. 1992, A&A, 259, L46
Lee, Y.-W., & Demarque, P. 1990, ApJS, 73, 709
Martin, W. C. 1938, Leiden Annalen, Vol. XVII, Part 2
Nemec, J. M. 1985, AJ, 90, 240
Nemec, J. M., & Clement, C. M. 1989, AJ, 98, 860
Petersen, J. O. 1984, A&A, 139, 496
Rogers, F. J., & Iglesias, C. A. 1992, ApJS, 79, 507
Rood, R. T. 1990, in Confrontation Between Stellar Pulsation and Evolution, ed. C. Cacciari & G. Clementini (San Francisco: ASP), 11
Saha, A., Freedman, W. L., Hoessel, J. G., & Mossman, A. E. 1992, AJ, 104, 1072
Sandage, A. 1982, ApJ, 350, 631
Sandage, A., & Cacciari, C. 1990, ApJ, 350, 631
Simon, N. R. 1985, ApJ, 299, 723
———. 1988, in Pulsation and Mass Loss in Stars, ed. R. Stalio & L. A. Willson (Dordrecht: Reidel), 27
———. 1989, ApJ, 343, L17
———. 1990a, MNRAS, 246, 70 (S90a)
———. 1990b, ApJ, 360, 199
Simon, N. R., & Aikawa, T. 1986, ApJ, 304, 249
Simon, N. R., & Clement, C. M. 1993, in New Perspectives on Stellar Pulsation and Pulsating Variable Stars, ed. J. M. Nemec & J. M. Matthews (Cambridge: Cambridge Univ. Press), 304
Walker, A. R. 1990, AJ, 100, 1532
———. 1992a, AJ, 103, 1166
———. 1992b, preprint

© American Astronomical Society • Provided by the NASA Astrophysics Data System